Journal of Solid Mechanics Vol. 13, No. 3 (2021) pp. 269-285
DOI: 10.22034/jsm.2020.678358

Dynamic Response of Bi-Directional Functionally Graded Materials (BDFGMs) Beams Rested on Visco-Pasternak Foundation Under Periodic Axial Force

A.A. Ghorbanpour Arani *, Sh. Niknejad, A.A. Abbasian Arani

Mechanical Engineering Faculty, University of Kashan, Kashan, Iran

Received 23 March 2021; accepted 22 May 2021

ABSTRACT

Since the temperature or stress distribution in some advanced machines such as modern aerospace shuttles and craft develops in two or three directions, the need for a new type of FGMs is felt whose properties vary in two or three directions. On the other hand, dynamic buckling behavior of structures is a complicated phenomenon which should be investigated through the response of equations of motion. In this paper, dynamic response of beams composed of bi-directional functionally graded materials (BDFGMs) rested on visco-Pasternak foundation under periodic axial force is investigated. Material properties of BDFGMs beam vary continuously in both the thickness and longitudinal directions based on the two types of analytical functions (e.g. exponential and power law distributions). Hamilton's principle is employed to derive the equations of motion of BDFGMs beam according to the Euler-Bernoulli and Timoshenko beam theories. Then, the generalized differential quadrature (GDQ) method in conjunction with the Bolotin method is used to solve the differential equations of motion under different boundary conditions. It is observed that a good agreement between the present work and the literature result. Various parametric investigations are performed for the effects of the gradient index, length-to-thickness ratio and viscoelastic foundation coefficients on the dynamic stability region of BDFGMs beam. The results show that the influence of gradient index of material properties along the thickness direction is greater than gradient index along the longitudinal direction on the dynamic stability of BDFGMs beam for both exponential and power law distributions.

Keywords : Dynamic stability; BDFGM; Visco-Pasternak foundation; Periodic axial force.

1 INTRODUCTION

DYNAMIC buckling behavior of structures is a complicated phenomenon which should be investigated

*Corresponding author. Tel.: +98 3155912450; Fax.: +98 3155912424.
E-mail address: a.ghorban.arani@gmail.com (A.A. Ghorbanpour Arani)

through the response of equations of motion. Selection of proper criterion is the most important factor in description of a dynamically buckled structure. On the other hand, when the structure is slender and lightweight, the need to study on the dynamic buckling problem would be necessary. At the first time, Bolotin [1] introduced dynamic stability in elastic systems. Also, Simitses [2, 3] presented a wealth review on the concept of dynamic buckling and its applications to solid structures. In recent years, different works are done in the field of dynamic stability and buckling of columns [4], beams [5-20], plates [21-23], shells [24-26] and etc. Iwatsubo et al. [4] solved the governing equations of motion for columns using Mathieu equations in conjunction with the Galerkin method and then, he determined the influences of internal and external damping on the regions of instability of the columns. Abbas and Thomas [5], Aristizabal-Ochoa [6], Briseghella et al. [7] and Ozturk and Sabuncu [8] employed finite element method (FEM) to investigate the dynamic stability of beams. The stability parameter of simply supported and clamped beams were calculated by Shastry and Rao [9] for different locations of two symmetrically placed intermediate supports. Li [10] developed a unified approach to analyze static and dynamic behavior of functionally graded material (FGM) beams of Euler-Bernoulli, Timoshenko and Rayleigh types. Ke and Wang [11] presented dynamic stability of microbeams made of FGMs based on the modified couple stress theory (MCST) and Timoshenko beam theory. They assumed that the material properties of FGM vary in the thickness direction of beam based on the Mori–Tanaka homogenization technique. Mohanty et al. [12] studied the static and dynamic behavior of FG ordinary beam and FG sandwich beam for pined-pined end condition. Based on the exponential and power law models which consider the variation of material properties through the thickness, they utilized first order shear deformation theory (FSDT) to model beam and used FEM for the analysis. Fu et al. [13] obtained the nonlinear governing equation for the FGM beam with two clamped ends and surface-bonded piezoelectric actuators by the Hamilton's principle. Also, they studied the thermo-piezoelectric buckling, nonlinear free vibration and dynamic stability for this system, subjected to one-dimensional steady heat conduction in the thickness direction. Static and dynamic stability of a FG micro-beam based on MCST subjected to nonlinear electrostatic pressure and thermal changes regarding convection and radiation were investigated by Zamanzadeh et al. [14]. They obtained the static pull-in voltages in presence of temperature changes using step-by-step linearization method (SSLM) and the dynamic pull-in voltages by adapting Runge–Kutta approach. Ke et al. [15] presented dynamic stability analysis of FG nanocomposite beams reinforced by FG single-walled carbon nanotubes (SWCNTs) based on Timoshenko beam theory. They employed the rule of mixture to estimate the material properties of FG carbon nanotube-reinforced composites. Ghorbanpour Arani et al. [16] investigated dynamic stability of double-walled boron nitride nanotube conveying viscous fluid using Timoshenko beam theory based on nonlocal piezo elasticity theory. They applied the mechanical harmonic excitation and thermal loadings on double-walled boron nitride nanotube with zero electrical boundary condition and derived the governing equations with regard to von Kármán geometric nonlinearity. The nonlinear dynamic buckling and imperfection sensitivity of the FGM Timoshenko beam under sudden uniform temperature rise were presented by Ghiasian et al. [17]. They employed the Budiansky–Roth criterion to distinguish the unbounded motion type of dynamic buckling and observed that no dynamic buckling occurs based on it for beams with stable post-buckling equilibrium path. Xu et al. [18] developed the random factor method for the stochastic dynamic characteristics analysis of beams that are made of FGM with random constituent material properties. They assumed that the effective material properties of FGM beams vary continuously through the thickness or axial directions according to the power law distribution. Shegokara and Lal [19] studied the dynamic instability response of un-damped elastically supported piezoelectric FG beams subjected to in-plane static and dynamic periodic thermo-mechanical loadings with uncertain system properties. They derived the nonlinear governing equations based on higher order shear deformation beam theory (HSDT) with von-Karman strain kinematics. Recently, Saffari et al. [20] investigated dynamic stability of FG nanobeam under axial and thermal loadings using nonlocal Timoshenko beam theory. Also, they considered surface stress effects according to Gurtin-Murdoch continuum theory. In 1984 during a space vehicle project, some Japanese material scientists presented the concept of FGMs. FGMs are made of two (or more) different materials which their properties such as mechanical strength, thermal conductivity and electrical conductivity vary continuously in a desired direction from point to point. It is the one of the most important advantages of FGMs against the classical laminated composites. Nowadays, the use of FGMs [27-32], composites [33-35] and sandwich structures [36-42] in many applications of engineering are developed such as aircrafts, space vehicles, defense industries, electronics and biomedical sectors due to their superior mechanical and thermal properties. It is seen from the literature survey that there are many worthwhile works in the case of conventional FG structures whose material properties vary in only one direction. Since the temperature or stress distribution in some advanced machines such as modern aerospace shuttles and craft develops in two or three directions, the need for a new type of FGMs is felt whose properties vary in two or three directions. Therefore, the number of researches about structures consist of BDFGMs is still very limited. On the other hand, there are no significant researches about the dynamic stability of beams composed of bi-directional functionally graded materials (BDFGMs) in above works.

In this article, the dynamic stability of BDFGMs beam rested on visco-Pasternak foundation under periodic axial force is studied. Material properties of BDFGMs beam vary continuously in both axial and thickness directions according to the exponential and power law distributions. By considering the Euler-Bernoulli and Timoshenko beam theories, the equations of motion of present system are obtained based on the Hamilton's principle and solved numerically by the generalized differential quadrature (GDQ) method and the Bolotin method under different boundary conditions.

2 BI-DIRECTIONAL DUNCTIONALLY GRADED MATERIAL (BDFGM)

As shown in Fig. 1, consider a BDFGM beam with length *L*, width *b* and thickness *h* which is rested on visco-Pasternak foundation includes springs (K_w), dampers (C_d) and shear layer (K_G). Also, the beam is exposed to a periodic axial force *F(t)*. It should be noted that the origin of the coordinate system is chosen at the midpoint of the beam.

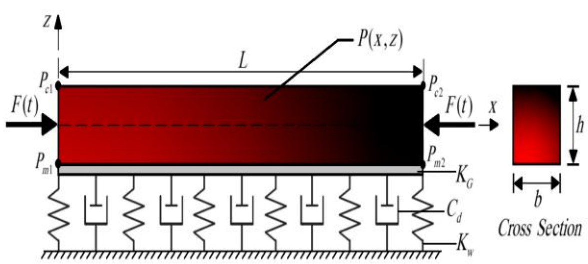

Fig.1
Geometry of a BDFGM beam rested on visco-Pasternak foundation subjected to a periodic axial force *F(t)*.

2.1 Power law distribution

In this paper, it is assumed the beam is made of four different materials, and thus, the effective material properties in points P_{m1}, P_{m2}, P_{c1} and P_{c2}, are specified in Fig. 1. Also, Young's modulus *E*, shear modulus *G*, and mass density ρ (except for Poisson's ratio υ) vary in both the thickness and longitudinal directions for BDFGM beam. Therefore, the effective material properties of BDFGM beam can be obtained by applying the rule of mixture as follows [43]:

$$P(x,z)=V_{c1}P_{c1}+V_{c2}P_{c2}+V_{m1}P_{m1}+V_{m2}P_{m2}, \tag{1}$$

where V is the volume fraction of materials. Based on the power law distribution, the volume fractions can be defined as:

$$\begin{aligned} &V_{c1}=\left(\frac{z}{h}+\frac{1}{2}\right)^{n_z}\left[1-\left(\frac{x}{L}\right)^{n_x}\right], V_{c2}=\left(\frac{z}{h}+\frac{1}{2}\right)^{n_z}\left(\frac{x}{L}\right)^{n_x},\\ &V_{m1}=\left[1-\left(\frac{z}{h}+\frac{1}{2}\right)^{n_z}\right]\left[1-\left(\frac{x}{L}\right)^{n_x}\right], V_{m2}=\left[1-\left(\frac{z}{h}+\frac{1}{2}\right)^{n_z}\right]\left(\frac{x}{L}\right)^{n_x}, \end{aligned} \tag{2}$$

where n_x and n_z are the gradient indexes which dictate the material variation profile through in *x* and *z* directions, respectively. Substituting Eq. (2) into Eq. (1), the effective material properties can be found by:

$$P(x,z)=\left[P_{m1}+\left(P_{c1}-P_{m1}\right)\left(\frac{z}{h}+\frac{1}{2}\right)^{n_z}\right]\left[1-\left(\frac{x}{L}\right)^{n_x}\right]+\left[P_{m2}+\left(P_{c2}-P_{m2}\right)\left(\frac{z}{h}+\frac{1}{2}\right)^{n_z}\right]\left(\frac{x}{L}\right)^{n_x}, \tag{3}$$

2.2 Exponential distribution

Now, consider that the effective material properties of BDFGMs beam obey an exponential distribution through the thickness and length of the beam as following form [44]:

$$P\left(x,z\right)=\frac{P_{m1}}{1-e}\left[\exp\left(\frac{x}{L}\right)^{n_x}-e\right]\exp\left[\ln\left(\frac{P_{c1}}{P_{m1}}\right)\left(\frac{1}{2}+\frac{z}{h}\right)^{n_z}\right]$$
$$+\frac{P_{m2}}{1-e}\left[1-\exp\left(\frac{x}{L}\right)^{n_x}\right]\exp\left[\ln\left(\frac{P_{c2}}{P_{m2}}\right)\left(\frac{1}{2}+\frac{z}{h}\right)^{n_z}\right], \tag{4}$$

It should be noted that by setting $n_x = n_y = 0$, the beam becomes homogeneous in both exponential and power law distributions.

3 GOVERNING EQUATIONS OF MOTION

Based on Timoshenko beam theory, the displacement field of BDFGMs beam can be given by:

$$\begin{aligned}\bar{u}\left(x,z,t\right)&=u\left(x,t\right)+z\,\varphi\left(x,t\right),\\ \bar{w}\left(x,z,t\right)&=w\left(x,t\right),\end{aligned} \tag{5}$$

In which, *u* and *w* represent the axial and transverse displacements of the point on the *x*-axis, respectively, and φ is the rotation of the cross section about the *y*- axis.

The kinematic relations for Timoshenko beam can be expressed as follows:

$$\begin{aligned}\varepsilon_{xx}&=\frac{\partial\bar{u}}{\partial x}=\frac{\partial u}{\partial x}+z\,\frac{\partial\varphi}{\partial x},\\ \gamma_{xz}&=\frac{\partial\bar{u}}{\partial z}+\frac{\partial\bar{w}}{\partial x}=\frac{\partial w}{\partial x}+\varphi,\end{aligned} \tag{6}$$

where ε_{xx} is normal strain and γ_{xz} is the shear strain. Thus, the stress-strain relations according to the Hook's law can be written as:

$$\begin{aligned}\sigma_{xx}&=E\left(x,z\right)\varepsilon_{xx},\\ \tau_{xz}&=kG\left(x,z\right)\gamma_{xz},\end{aligned} \tag{7}$$

where σ_{xx} and τ_{xz} are the normal and shear stresses, respectively. Also, $G(x,z)=\frac{1}{2}\frac{E(x,z)}{1+\upsilon}$. In addition, *k* is shear correction factor and equal to $\frac{5+5\upsilon}{6+6\upsilon}$ for Timoshenko beam.

Based on the Hamilton's principle, which states that the motion of an elastic structure during the time interval $t_1 < t < t_2$ is such that the time integral of the total dynamics potential is extremum:

$$\int_{t_1}^{t_2}\delta\left(T-U+W_{ext}\right)dt=0, \tag{8}$$

In which, *U*, *T* and W_{ext} are the strain energy, kinetic energy and work done by external forces, respectively. The virtual strain energy can be calculated as:

$$\delta U = \int_{\forall} \left(\sigma_{ij}\, \delta\varepsilon_{ij} \right) d\forall = \int_{\forall} \left(\sigma_{xx}\, \delta\varepsilon_{xx} + \tau_{xz}\, \delta\gamma_{xz} \right) d\forall, \tag{9}$$

where $\forall$ is the volume of beam. Substituting Eqs. (6) and (7) into Eq. (9) yields:

$$\delta U = \int_0^L \left(N_{TBT} \frac{\partial \delta u}{\partial x} + M_{TBT} \frac{\partial \delta \varphi}{\partial x} + Q_{TBT} \left(\frac{\partial \delta w}{\partial x} + \delta\varphi \right) \right) dx, \tag{10}$$

where subscript *TBT* refers to Timoshenko beam theory. Also, *N*, *M* and *Q* represent the axial force, bending moment and shear force, respectively. Generally, this term can be obtained from:

$$N = \int_{-\frac{h}{2}}^{\frac{h}{2}} \int_{-\frac{b}{2}}^{\frac{b}{2}} \sigma_{xx}\, dydz, \quad M = \int_{-\frac{h}{2}}^{\frac{h}{2}} \int_{-\frac{b}{2}}^{\frac{b}{2}} z\, \sigma_{xx}\, dydz, \quad Q = \int_{-\frac{h}{2}}^{\frac{h}{2}} \int_{-\frac{b}{2}}^{\frac{b}{2}} \tau_{xz}\, dydz, \tag{11}$$

The kinetic energy for a beam can be written as:

$$T = \frac{1}{2} \int_{\forall} \rho(x,z) \left[\left(\frac{\partial \bar{u}}{\partial t} \right)^2 + \left(\frac{\partial \bar{w}}{\partial t} \right)^2 \right] d\forall, \tag{12}$$

By substituting Eq. (5) into Eq. (12), for Timoshenko beam, the virtual kinetic energy can be expressed as follows:

$$\delta T = \int_0^L \left[I_0 \frac{\partial u}{\partial t} \frac{\partial \delta u}{\partial t} + I_0 \frac{\partial w}{\partial t} \frac{\partial \delta w}{\partial t} + I_1 \left(\frac{\partial \varphi}{\partial t} \frac{\partial \delta u}{\partial t} + \frac{\partial u}{\partial t} \frac{\partial \delta \varphi}{\partial t} \right) + I_2 \frac{\partial \varphi}{\partial t} \frac{\partial \delta \varphi}{\partial t} \right] dx, \tag{13}$$

where

$$I_{0,1,2} = \int_{-\frac{h}{2}}^{\frac{h}{2}} \int_{-\frac{b}{2}}^{\frac{b}{2}} \rho(x,z) \left(1, z, z^2 \right) dydz. \tag{14}$$

The external work variation done by visco-Pasternak foundation [45] and periodic axial forces [46] can be given by:

$$\delta W_{ext} = \int_0^L \left[F_f\, \delta w - F(t) \frac{\partial w}{\partial x} \frac{\partial \delta w}{\partial x} \right] dx, \tag{15}$$

where

$$\begin{aligned} F_f &= -K_w w + K_G \frac{\partial^2 w}{\partial x^2} - C_d \frac{\partial w}{\partial t}, \\ F(t) &= N_{static} + N_{dynamic} \cos(\Omega t) = \alpha N_{cr} + \beta N_{cr} \cos(\Omega t), \end{aligned} \tag{16}$$

In which, α and β are static and dynamic load factors, respectively, and Ω is parametric resonance. By Substituting Eqs. (10), (13) and (15) into Eq. (8) and putting the coefficients of δu, δw and $\delta\varphi$ to zero, the equations of motion can be determined as follows:

$$\frac{\partial N_{TBT}}{\partial x} = I_0 \frac{\partial^2 u}{\partial t^2} + I_1 \frac{\partial^2 \varphi}{\partial t^2}, \tag{17a}$$

$$\frac{\partial Q_{TBT}}{\partial x} + F_f + F(t)\frac{\partial^2 w}{\partial x^2} = I_0 \frac{\partial^2 w}{\partial t^2}, \tag{17b}$$

$$\frac{\partial M_{TBT}}{\partial x} - Q_{TBT} = I_1 \frac{\partial^2 u}{\partial t^2} + I_2 \frac{\partial^2 \varphi}{\partial t^2}, \tag{17c}$$

Moreover, the appropriate boundary conditions given by Eq. (8) can be written as:
Clamped

$$u = w = \varphi = 0, \tag{18a}$$

Simple

$$u = w = 0,\ M_{TBT} = 0, \tag{18b}$$

Free

$$N_{TBT} = M_{TBT} = 0,\ Q_{TBT} + F(t)\frac{\partial w}{\partial x} = 0, \tag{18c}$$

Substituting Eq. (7) into Eq. (11), the normal force-strain, the bending moment-strain and the shear force-strain relations based on Timoshenko beam theory can be given by:

$$N_{TBM} = A_0 \frac{\partial u}{\partial x} + A_1 \frac{\partial \varphi}{\partial x}, \tag{19a}$$

$$M_{TBM} = A_1 \frac{\partial u}{\partial x} + A_2 \frac{\partial \varphi}{\partial x}, \tag{19b}$$

$$Q_{TBM} = A_3\left(\frac{\partial w}{\partial x} + \varphi\right), \tag{19c}$$

where

$$A_{0,1,2}(x) = \int_{-\frac{h}{2}}^{\frac{h}{2}}\int_{-\frac{b}{2}}^{\frac{b}{2}} E(x,z)\left(1,z,z^2\right)dydz,\ A_3(x) = \int_{-\frac{h}{2}}^{\frac{h}{2}}\int_{-\frac{b}{2}}^{\frac{b}{2}} kG(x,z)\,dydz, \tag{20}$$

The equations of motion of BDFGMs beam in terms of the displacements can be derived by substituting for *N*, *M* and *Q* from Eq. (19) into Eq. (17) as follows:

$$A_0 \frac{\partial^2 u}{\partial x^2} + \frac{dA_0}{dx}\frac{\partial u}{\partial x} + A_1 \frac{\partial^2 \varphi}{\partial x^2} + \frac{dA_1}{dx}\frac{\partial \varphi}{\partial x} = I_0 \frac{\partial^2 u}{\partial t^2} + I_1 \frac{\partial^2 \varphi}{\partial t^2}, \tag{21a}$$

$$A_3\left(\frac{\partial^2 w}{\partial x^2} + \frac{\partial \varphi}{\partial x}\right) + \frac{dA_3}{dx}\left(\frac{\partial w}{\partial x} + \varphi\right) - K_w w + K_G \frac{\partial^2 w}{\partial x^2} - C_d \frac{\partial w}{\partial t} + F(t)\frac{\partial^2 w}{\partial x^2} = I_0 \frac{\partial^2 w}{\partial t^2}, \tag{21b}$$

$$A_1\frac{\partial^2 u}{\partial x^2}+\frac{dA_1}{dx}\frac{\partial u}{\partial x}+A_2\frac{\partial^2\varphi}{\partial x^2}+\frac{dA_2}{dx}\frac{\partial\varphi}{\partial x}-A_3\left(\frac{\partial w}{\partial x}+\varphi\right)=I_1\frac{\partial^2 u}{\partial t^2}+I_2\frac{\partial^2\varphi}{\partial t^2}, \tag{21c}$$

Also, the appropriate boundary conditions in terms of the displacements can be given by:
Clamped

$$u=w=\varphi=0, \tag{22a}$$

Simple

$$u=w=0,\ A_1\frac{\partial u}{\partial x}+A_2\frac{\partial\varphi}{\partial x}=0, \tag{22b}$$

Free

$$\frac{\partial u}{\partial x}=\frac{\partial\varphi}{\partial x}=0,\ A_3\left(\frac{\partial w}{\partial x}+\varphi\right)+F(t)\frac{\partial w}{\partial x}=0 \tag{22c}$$

In order to derive the equations of motion based on the Euler–Bernoulli beam theory, the displacement field at any point of the beam can be defined as:

$$\begin{aligned}\bar{u}(x,z,t)&=u(x,t)-z\,\frac{\partial w(x,t)}{\partial x},\\ \bar{w}(x,z,t)&=w(x,t),\end{aligned} \tag{23}$$

The only nonzero strain and stress are:

$$\begin{aligned}\varepsilon_{xx}&=\frac{\partial\bar{u}}{\partial x}=\frac{\partial u}{\partial x}-z\,\frac{\partial^2 w}{\partial x^2},\\ \sigma_{xx}&=E(x,z)\,\varepsilon_{xx},\end{aligned} \tag{24}$$

For this case, the strain energy and kinetic energy can be written as:

$$\delta U=\int_0^L\left(N_{EBT}\frac{\partial\delta u}{\partial x}-M_{EBT}\frac{\partial^2\delta w}{\partial x^2}\right)dx, \tag{25}$$

$$\delta T=\int_0^L\left[I_0\frac{\partial u}{\partial t}\frac{\partial\delta u}{\partial t}+I_0\frac{\partial w}{\partial t}\frac{\partial\delta w}{\partial t}-I_1\left(\frac{\partial^2 w}{\partial t\,\partial x}\frac{\partial\delta u}{\partial t}+\frac{\partial u}{\partial t}\frac{\partial^2\delta w}{\partial t\,\partial x}\right)+I_2\frac{\partial^2 w}{\partial t\,\partial x}\frac{\partial^2\delta w}{\partial t\,\partial x}\right]dx, \tag{26}$$

where subscript *EBT* refers to Euler–Bernoulli beam theory. Using the Euler–Bernoulli beam theory, the equations of motion and boundary conditions of BDFGMs beam can be obtained by substituting Eqs. (15), (25) and (26) into Eq. (8) and setting the coefficients of δu and δw to zero as follows:

$$\frac{\partial N_{EBT}}{\partial x}=I_0\frac{\partial^2 u}{\partial t^2}-I_1\frac{\partial^3 w}{\partial t^2\partial x}, \tag{27a}$$

$$\frac{\partial^2 M_{EBT}}{\partial x^2}+F_f+F(t)\frac{\partial^2 w}{\partial x^2}=I_0\frac{\partial^2 w}{\partial t^2}+I_1\frac{\partial^3 u}{\partial t^2\partial x}-I_2\frac{\partial^4 w}{\partial t^2\partial x^2}, \tag{27b}$$

Clamped

$$u = w = 0,\ \frac{\partial w}{\partial x} = 0, \tag{28a}$$

Simple

$$u = w = 0,\ M_{EBT} = 0, \tag{28b}$$

Free

$$N_{EBT} = M_{EBT} = 0,\ \frac{\partial M_{EBT}}{\partial x} - F(t)\frac{\partial w}{\partial x} = 0, \tag{28c}$$

Substituting Eq. (24) into Eq. (11), the normal force-strain and the bending moment-strain relations based on the Euler–Bernoulli beam theory can be expressed as following form:

$$N_{EBT} = A_0\frac{\partial u}{\partial x} - A_1\frac{\partial^2 w}{\partial x^2}, \tag{29a}$$

$$M_{EBT} = -A_1\frac{\partial u}{\partial x} + A_2\frac{\partial^2 w}{\partial x^2}, \tag{29b}$$

By substituting Eq. (29) into Eq. (27), the equations of motion and boundary conditions in terms of the displacements can be obtained as:

$$A_0\frac{\partial^2 u}{\partial x^2} + \frac{dA_0}{dx}\frac{\partial u}{\partial x} - A_1\frac{\partial^3 w}{\partial x^3} - \frac{dA_1}{dx}\frac{\partial^2 w}{\partial x^2} = I_0\frac{\partial^2 u}{\partial t^2} - I_1\frac{\partial^3 w}{\partial t^2 \partial x}, \tag{30a}$$

$$\begin{aligned}&A_1\frac{\partial^3 u}{\partial x^3} + 2\frac{dA_1}{dx}\frac{\partial^2 u}{\partial x^2} + \frac{d^2 A_1}{dx^2}\frac{\partial u}{\partial x} - A_2\frac{\partial^4 w}{\partial x^4} - 2\frac{dA_2}{dx}\frac{\partial^3 w}{\partial x^3} - \frac{d^2 A_2}{dx^2}\frac{\partial^2 w}{\partial x^2}\\ &-K_w w + K_G\frac{\partial^2 w}{\partial x^2} - C_d\frac{\partial w}{\partial t} + F\left(t\right)\frac{\partial^2 w}{\partial x^2} = I_0\frac{\partial^2 w}{\partial t^2} + I_1\frac{\partial^3 u}{\partial t^2 \partial x} - I_2\frac{\partial^4 w}{\partial t^2 \partial x^2},\end{aligned} \tag{30b}$$

Clamped

$$u = w = 0,\ \frac{\partial w}{\partial x} = 0, \tag{31a}$$

Simple

$$u = w = 0,\ A_1\frac{\partial u}{\partial x} - A_2\frac{\partial^2 w}{\partial x^2} = 0, \tag{31b}$$

Free

$$\frac{\partial u}{\partial x} = 0,\ \frac{\partial^2 w}{\partial x^2} = 0,\ A_1\frac{\partial^2 u}{\partial x^2} - A_2\frac{\partial^3 w}{\partial x^3} + F(t)\frac{\partial w}{\partial x} = 0. \tag{31c}$$

4 SOLUTION METHOD

In order to solve the governing differential Eqs. (30) and the associated boundary conditions (31), the GDQ method [47, 48] is employed to determine the dynamic stability characteristics of BDFGMs beam. According to these methods, the partial derivative of a function with respect to spatial variables at a given discrete point is evaluated as:

$$\frac{\partial^r}{\partial x^r}\{u,w,\varphi\}_{x=x_i}=\sum_{j=1}^{N}A_{ij}^{(r)}\{u_j(x_i),w_j(x_i),\varphi_j(x_i)\}, \tag{32}$$

where N is the number of total discrete grid points along the x- axis and $A_{ij}^{(r)}$ are the weighting coefficients associated with the *rth* order of derivative. Based on the Lagrangian polynomial interpolation, the weighting coefficients for the first derivative (i.e., $r = 1$) can be approximated by:

$$\begin{cases} A_{ij}^{(1)}=\prod\limits_{k=1,k\neq i,j}^{N}(x_i-x_k)\Big/\prod\limits_{k=1,k\neq j}^{N}(x_j-x_k) & (i\neq j) \\ A_{ij}^{(1)}=\prod\limits_{k=1,k\neq i}^{N}\dfrac{1}{(x_i-x_k)} & (i=j) \end{cases} \quad \text{for } i,j=1,2,\dots,N \tag{33}$$

Similarly, higher order of derivative can be calculated as:

$$A_{ij}^{(r+1)}=\sum_{k=1}^{N}A_{ik}^{(1)}A_{kj}^{(r)} \quad for\; i,j=1,2,\dots,N \tag{34}$$

On the other hand, the differential quadrature solutions usually deliver more accurate results with nonuniformly spaced sampling. A well accepted kind of sampling points can be obtained by the Chebyshev–Gauss–Lobatto normalized distribution equation:

$$x_i=\frac{1}{2}\left[1-\cos\left(\pi\frac{i-1}{N-1}\right)\right] \quad for\; i=1,2,\dots,N \tag{35}$$

By inserting Eq. (32) into Eqs. (21, 22 and 30, 31) and implementing the GDQ method, a set of discretized governing equations and the boundary conditions can be found in the matrix form as follows:

$$[M]\{\ddot{X}\}+[C]\{\dot{X}\}+([K]+P(t)[K_P])\{X\}=\{0\}, \tag{36}$$

In which M, C, K and K_P represent the mass, damping, stiffness and geometrical stiffness matrices, respectively. Also, X is the displacement vector ($X=u,\varphi,w$). In 1964, Bolotin [1] suggested a method in order to determine the dynamic instability region. He indicates that the first instability region is wider than other regions and the structural damping becomes neutralized in higher regions. Based on this method, the displacement vector can be expressed in the Fourier series with the period *2T* as following form:

$$X=\sum_{k=1,3,5,\dots}^{\infty}\left(a_k\sin\frac{k\Omega t}{2}+b_k\cos\frac{k\Omega t}{2}\right), \tag{37}$$

where a_k and b_k are unknown constants. By introducing Eq. (37) into Eq. (36) and setting the coefficients of each sine and cosine as well as the sum of the constant terms to zero, yield:

$$\left|[K]-\alpha P_{cr}[K_P]\pm P_{cr}\frac{\beta}{2}[K_P]\mp\frac{\Omega}{2}[C]-\frac{\Omega^2}{4}[M]\right|=0. \tag{38}$$

Eq. (38) can be solved based on the eigenvalue problems, and the dynamic instability regions will obtain by plotting the variation of Ω with respect to β .

5 NUMERICAL RESULTS AND DISCUSSION

In this section, the influences of various parameters such as the gradient index of exponential and power law distributions, length-to-thickness ratio, different boundary conditions and viscoelastic foundation coefficients on the dynamic stability region of beam are discussed in details. Silicon (Si_3N_4), zirconia (ZrO_2), stainless steel (SUS304) and titanium (Ti-6Al-4V) with the material properties at room temperature given in Ref. [49, 50] are employed as ceramic1, ceramic2, metal1 and metal2, respectively. Also, In order to obtain the results of this research, other parameters are selected as follows:

$$L=2m,\ h/L=0.04,\ n_x=n_z=2,\ \upsilon=0.3,\ K_w=10^4\,N/m^3,\ K_G=10^3\,N/m,\ C_d=50Ns/m^3,\ \alpha=0.2$$

In addition, CC boundary condition is considered for BDFGMs beam except for the cases to be mentioned.

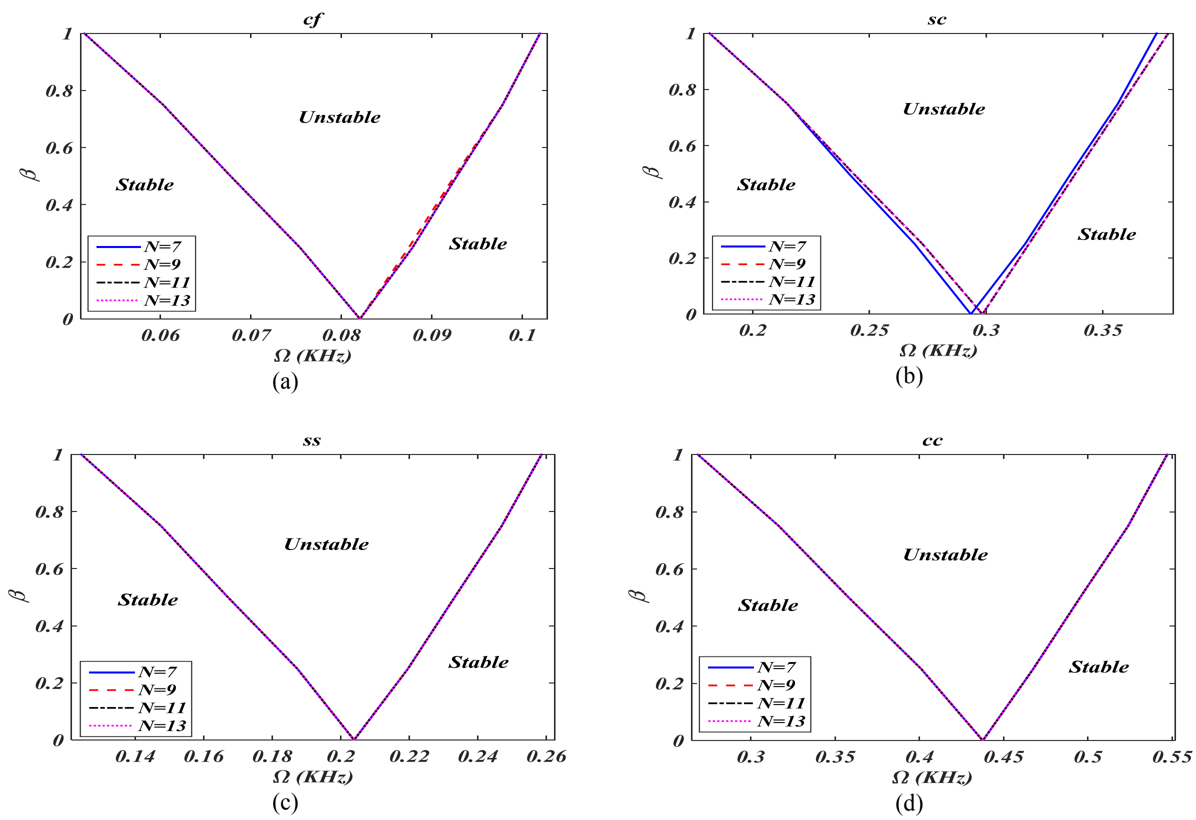

Fig.2
The convergence of grid points of the GDQ method for a) CF, b) SS, c) SC, d) CC boundary conditions.

Fig. 2 indicates the convergence of grid points of the GDQ method used to evaluate the stability of the BDFGMs beam with arbitrary boundary conditions. The results show that the convergence occurs quickly for different boundary conditions and thus, N=11 selected to obtain the numerical results. This pattern of convergence of the numerical technique reflects its efficiency and reliability.

By converging the grid points in N=11*,* validation and convergence of the derived formulation must be checked now. For this purpose, in Table 1, the fundamental frequency parameters of BDFGMs beam with SS boundary conditions are compared with Ref. [51] where a finite element formulation based on Timoshenko beam theory was utilized. As can be seen, very good agreement between the results of present paper with Ref. [51].

Table 1
Comparison of fundamental frequency parameter ($\bar{\omega}=\omega\left(L^2/h\right)\sqrt{\rho_{Al}/E_{Al}}$) of BDFGMs beam with SS boundary conditions.

n_z	Source	n_x = 0	$\frac{1}{3}$	$\frac{1}{2}$	$\frac{5}{6}$	1	$\frac{4}{3}$	$\frac{3}{2}$	2
0	Present	3.3032	3.7383	3.9127	4.1986	4.3171	4.5167	4.6012	4.8079
	Ref. [51]	3.3018	3.7429	3.9148	4.1968	4.3139	4.5118	4.5956	4.8005
$\frac{1}{3}$	Present	3.2189	3.5518	3.6791	3.8759	3.9534	4.0792	4.1307	4.2526
	Ref. [51]	3.1542	3.5050	3.6305	3.8252	3.9022	4.0277	4.0792	4.2009
$\frac{1}{2}$	Present	3.1997	3.4978	3.6099	3.7797	3.8455	3.9511	3.9939	4.0943
	Ref. [51]	3.1068	3.4258	3.5397	3.7087	3.7745	3.8805	3.9236	4.0245
$\frac{5}{6}$	Present	3.1570	3.4080	3.4984	3.6308	3.6810	3.7601	3.7918	3.8655
	Ref. [51]	3.0504	3.3296	3.4206	3.5548	3.6059	3.6869	3.7194	3.7947
1	Present	3.1366	3.3720	3.4542	3.5730	3.6179	3.6881	3.7161	3.7811
	Ref. [51]	3.0359	3.2984	3.3819	3.5035	3.5495	3.6219	3.6508	3.7177

Based on Timoshenko and Euler-Bernoulli beam theories, the dynamic stability regions of BDFGMs beam for various boundary conditions are demonstrated in Fig. 3. As it can be seen from this figure, CC and CF boundary conditions have the highest and lowest parametric resonance. Also, the dynamic instability region for CC boundary condition is higher than that for other boundary conditions. Such trend is expected due to the higher local flexural rigidity and stability of clamped edge in comparison to, in order, simply supported and free edges. In addition, the results obtained by Timoshenko and Euler-Bernoulli beam theories are very close to each other, especially for thin beam. In the other words, the obtained results by Timoshenko and Euler-Bernoulli beam theories have small difference. The Euler-Bernoulli beam theory have good accuracy for slender or thin beam ($h/l<0.1$) and Timoshenko beam theory can be used for both thin and thick ($h/l>0.1$) beam. The dynamic stability regions of BDFGMs beam for various static load factor are shown in Fig. 4. It can be observed that by increasing static load factor, the dynamic instability region shifts to the left and increase. This is expected as the increase of α means the increase of the time independent component of the axial force which reduces the effective stiffness of the beam. In addition, the parametric resonance obtained by Timoshenko beam theory is lower than Euler-Bernoulli beam theory but the area of dynamic instability regions of two theories are very close to each other.

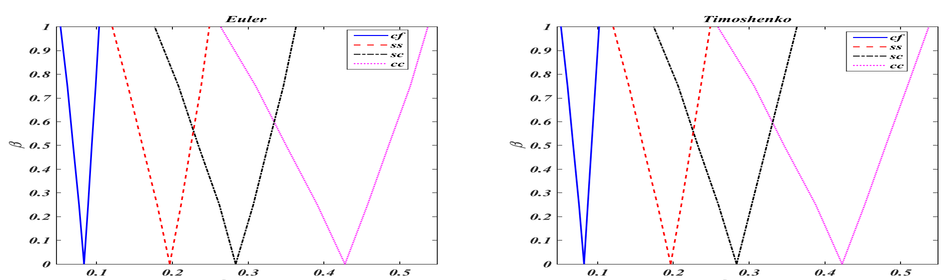

(a)

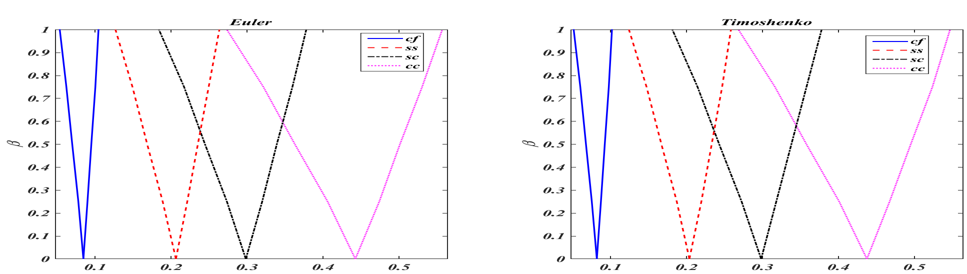

(b)

Fig.3
Effects of various boundary conditions on the dynamic stability of BDFGMs beam a) power law distribution, b) exponential distribution.

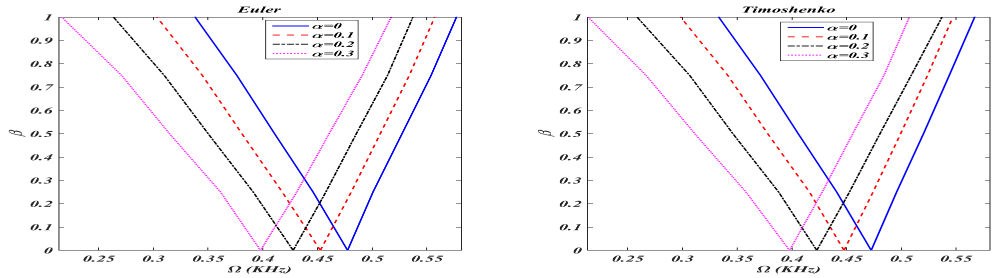

(a)

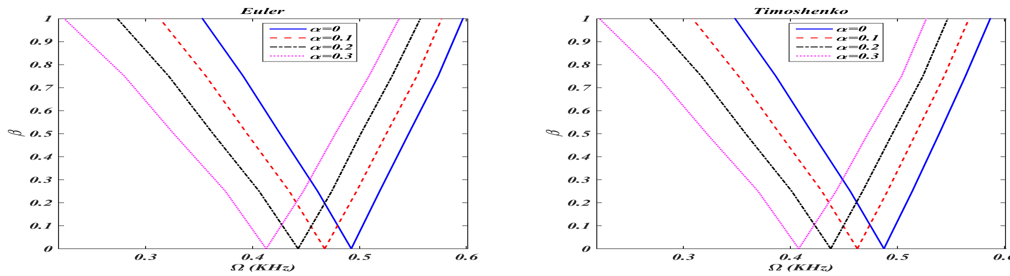

(b)

Fig.4
Effects of static load factor on the dynamic stability of BDFGMs beam a) Power law distribution, b) Exponential distribution.

Fig. 5 indicates the dynamic stability of BDFGMs beam for different gradient indexes through in x direction. According to this figure for both power law and exponential distributions, the parametric resonance increases with increasing of n_x and will be approximately constant for $n_x \geq 3$. Fig. 6 illustrates the dynamic stability of BDFGMs beam for different gradient indexes through in z direction. It can be found that by increasing n_z, the instability region decreases and moves to the side of smaller parametric resonance. Moreover, the influence of n_z is greater than n_x on the dynamic stability of present system by comparing Fig. 5 and Fig. 6.

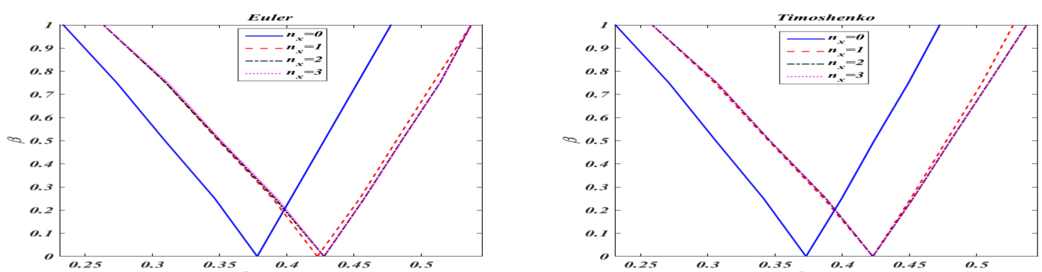

(a)

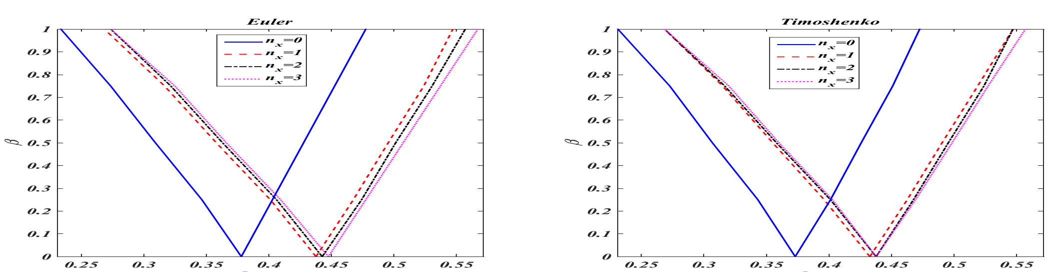

(b)

Fig.5
Effects of gradient index through in x direction (n_x) on the dynamic stability of BDFGMs beam a) Power law distribution, b) Exponential distribution.

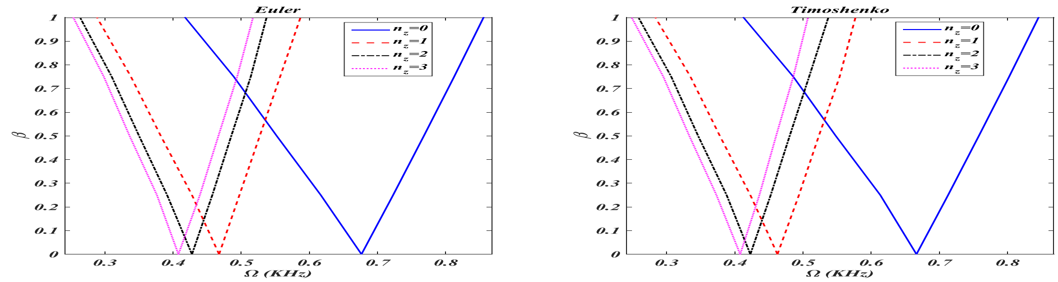

(a)

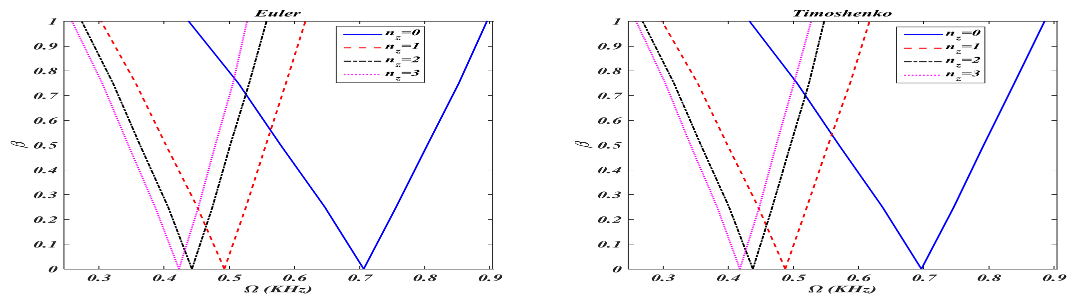

(b)

Fig.6
Effects of gradient index through in z direction (n_z) on the dynamic stability of BDFGMs beam a) Power law distribution, b) Exponential distribution.

The dynamic stability regions of BDFGMs beam for different thickness-to-length ratio are depicted in Fig. 7. It is obvious that by increasing thickness-to-length ratio, the system becomes more stable and thus, parametric resonance increases and shifts to the right side of figure.

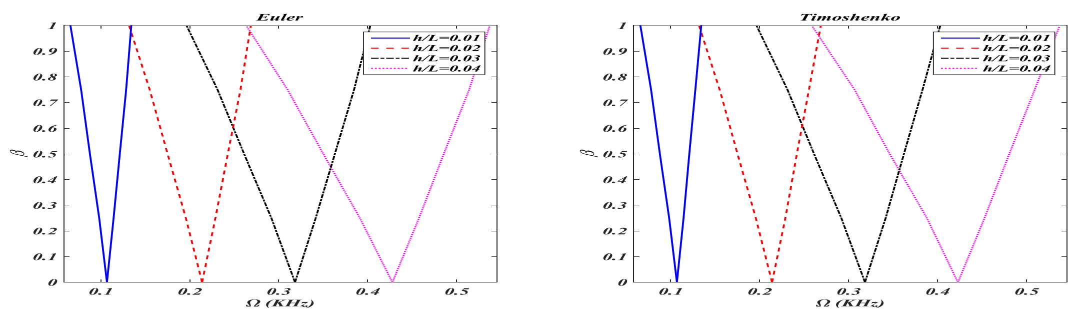

(a)

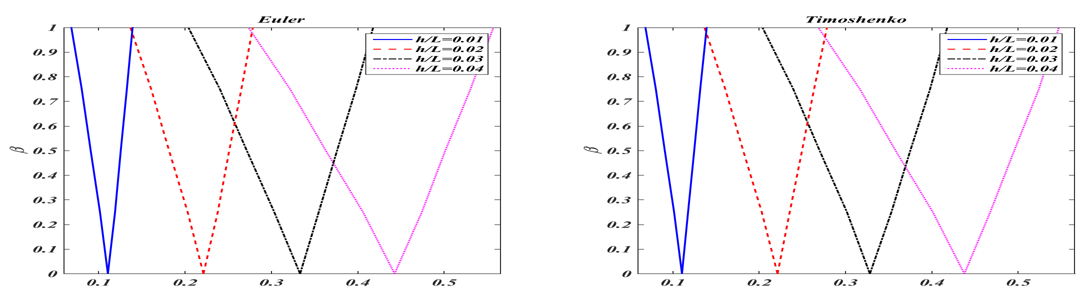

(b)

Fig.7
Effects of thickness-to-length ratio on the dynamic stability of BDFGMs beam a) Power law distribution, b) Exponential distribution.

Fig. 8 shows the effect of various foundation models on parametric resonance of BDFGMs beam. Four cases are considered to study the effect of foundation models, namely, case 1 (without foundation: $K_w = 0$, $K_G = 0, C_d = 0$), case 2 (Winkler foundation: $K_w = 50 MN/m^3, K_G = 0, C_d = 0$), case 3 (Pasternak foundation: $K_w = 50 MN/m^3$, $K_G = 10 MN/m, C_d = 0$) and case 4 (visco-Pasternak foundation: $K_w = 50 MN/m^3$, $K_G = 10 MN/m, C_d = 10 KNs/m^3$). By increasing Winkler and shear layer parameters, stiffness of system increases and thus, parametric resonance increases and the dynamic instability region shifts to the right. Moreover, variations of shear layer parameter have more influence than Winkler parameter on the displacement of dynamic stability regions. Also, it is evident that the dynamic instability region of BDFGMs beam reduces by increasing damping parameter. Generally, it can be observed that by adding the effects of elastic substrate to the system, parametric resonance increases and the dynamic instability region shifts to the right. As can be seen, the dynamic instability region of the Pasternak model due to consider the effects of normal stresses and the transverse shear deformation is higher than that of Winkler or visco-Pasternak one. Generally, putting BDFGMs beam in an elastic substrate leads to increase the stability and stiffness of system.

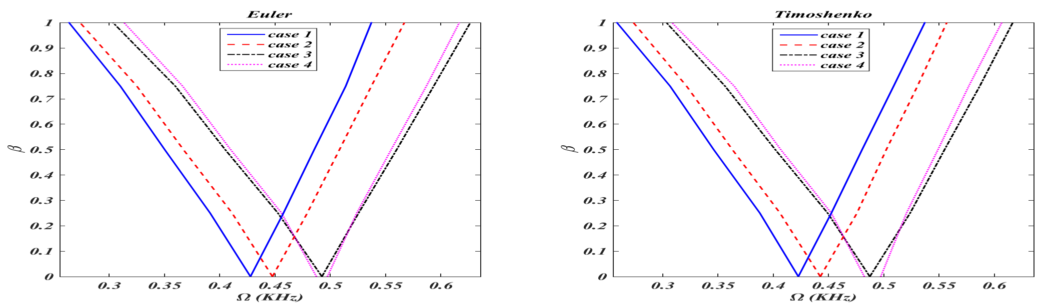

(a)

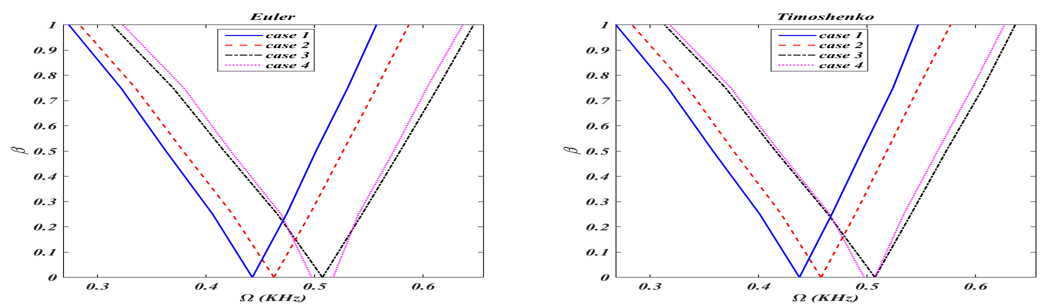

(b)

Fig.8
Effects of various foundation models on the dynamic stability of BDFGMs beam a) Power law distribution, b) Exponential distribution.

6 CONCLUSIONS

This paper studied the dynamic stability analysis of BDFGMs beams rested on visco-Pasternak foundation under periodic axial force. Two types of analytical functions include exponential and power law distributions considered to model the material properties of BDFGMs beam. The governing equations obtained by utilizing the Hamilton's principle according to the Euler-Bernoulli and Timoshenko beam theories and solved by GDQ method in conjunction with the Bolotin method. The results indicated that:

- The parametric resonance obtained by Timoshenko beam theory is lower than Euler-Bernoulli beam theory but the area of dynamic instability regions of two theories are very close to each other.
- The influence of gradient index of material properties along the thickness direction is greater than gradient index along the longitudinal direction on the dynamic stability of BDFGMs beam for both exponential and power law distributions.

- Considering exponential law model in order to determine the material properties of BDFGMs beam causes to obtain the larger parametric resonance in comparison with power law model.
- Putting BDFGMs beam in an elastic substrate makes the system more stable and stiffer.
- The dynamic instability region moves to the smaller parametric resonance by increasing static load factor.

ACKNOWLEDGMENTS

The author(s) disclosed receipt of the following financial support for the research, authorship, and/or publication of this article: The authors are grateful to the University of Kashan for supporting this work by Grant No. 574600/55.

REFERENCES

[1] Bolotin V.V., 1964, *The Dynamic Stability of Elastic Systems*, Holden-Day, San Francisco, CA.
[2] Simitses G.J., 1987, Instability of dynamically-loaded structures, *Applied Mechanics Reviews* **40**(10): 1403-1408.
[3] Simitses G.J., 1990, *Dynamic Stability of Suddenly Loaded Structures*, New York, Springer.
[4] Iwatsubo T., Sugiyama Y., Ogino S., 1974, Simple and combination resonances of columns under periodic axial loads, *Journal of Sound and Vibration* **33**: 211-221.
[5] Abbas B.A.H., Thomas J., 1978, Dynamic stability of Timoshenko beams resting on an elastic foundation, *Journal of Sound and Vibration* **60**: 33-44.
[6] Aristizabal-Ochoa J.D., 1993, Statics stability and vibration of non-prismatic beams and columns, *Journal of Sound and Vibration* **162**(3): 441-455.
[7] Briseghella L., Majorana C.E., Pellegrino C., 1998, Dynamic stability of elastic structures: a finite element approach, *Computers & Structures* **69**: 11-25.
[8] Ozturk H., Sabuncu M., 2005, Stability analysis of a cantilever composite beam on elastic support, *Composites Science and Technology* **65**: 1982-1995.
[9] Shastry B.P., Rao G.V., 1986, Dynamic stability of columns with two symmetrically placed intermediate supports, *Journal of Sound and Vibration* **104**(3): 524-527.
[10] Li X.F., 2008, A unified approach for analyzing static and dynamic behaviors of functionally graded Timoshenko and Euler-Bernaulli beams, *Journal of Sound and Vibration* **318**(4-5): 1210-1229.
[11] Ke L.L., Wang Y.S., 2011, Size effect on dynamic stability of functionally graded microbeams based on a modified couple stress theory, *Composites Structures* **93**(2): 342-350.
[12] Mohanty S.C., Dash R.R., Rout T., 2012, Static and dynamic stability analysis of a functionally graded Timoshenko beam, *International Journal of Structural Stability and Dynamics* **12**(4): 1250025-1250033.
[13] Fu Y., Wang J., Mao Y., 2012, Nonlinear analysis of buckling, free vibration and dynamic stability for the piezoelectric functionally graded beams in thermal environment, *Applied Mathematical Modelling* **36**(9): 4324-4340.
[14] Zamanzadeh M., Rezazadeh G., Jafarsadeghi-poornaki I., Shabani R., 2013, Static and dynamic stability modeling of a capacitive FGM micro-beam in presence of temperature changes, *Applied Mathematical Modelling* **37**(10-11): 6964-6978.
[15] Ke L.L., Yang J., Kitipornchai S. 2013, Dynamic stability of functionally graded carbon nanotube-reinforced composite beams, *Mechanics of Advanced Materials and Structures* **20**(1): 28-37.
[16] Ghorbanpour Arani A., Hashemian M., Kolahchi R., 2013, Nonlocal Timoshenko beam model for dynamic stability of double-walled boron nitride nanotubes conveying nanoflow, *Proceedings of the Institution of Mechanical Engineers, Part N, Journal of Nanomaterials, Nanoengineering and Nanosystems* **229**(1): 2-16.
[17] Ghiasian S.E., Kiani Y., Eslami M.R., 2015, Nonlinear thermal dynamic buckling of FGM beams, *European Journal of Mechanics - A/Solids* **54**: 232-242.
[18] Xu Y., Qian Y., Chen J., Song G., 2015, Stochastic dynamic characteristics of FGM beams with random material properties, *Composites Structures* **133**: 585-594.
[19] Shegokara N.L., Lal A., 2016, Stochastic dynamic instability response of piezoelectric functionally graded beams supported by elastic foundation, *Advances in Aircraft and Spacecraft Science* **3**(4): 471-502.
[20] Saffari S., Hashemian M., Toghraie D., 2017, Dynamic stability of functionally graded nanobeam based on nonlocal Timoshenko theory considering surface effects, *Physica B* **520**: 97-105.
[21] Ghorbanpour Arani A., Cheraghbak A., Kolahchi R., 2016, Dynamic buckling of FGM viscoelastic nano-plates resting on orthotropic elastic medium based on sinusoidal shear deformation theory, *Structural Engineering and Mechanics* **60**(3): 489-505.
[22] Ghorbanpour Arani A., Kolahchi R., Zarei M.S., 2015, Visco-surface-nonlocal piezoelasticity effects on nonlinear dynamic stability of graphene sheets integrated with ZnO sensors and actuators using refined zigzag theory, *Composites Structures* **132**: 506-526.
[23] Ghorbanpour Arani A., Jalaei M.H., 2016, Nonlocal dynamic response of embedded single-layered graphene sheet via analytical approach, *Journal of Engineering Mathematics* **98**(1): 129-144.

[24] Yao J.C., 1963, Dynamic stability of cylindrical shells under static and periodic axial and radial loads, *AIAA Journal of Air Transportation* **1**(6): 1391-1396.
[25] Nagai K., Yamaki N., 1978, Dynamic stability of circular cylindrical shells under periodic compressive forces, *Journal of Sound and Vibration* **58**(3): 425-441.
[26] Ghorbanpour Arani A., Mortazavi S.A., Khoddami Maraghi Z., 2015, Dynamic stability of nanocomposite viscoelastic cylindrical shells coating with a piezomagnetic layer conveying pulsating fluid flow, *Science and Engineering of Composite Materials* **24**(3): 401-414.
[27] Arefi M., Zenkour A.M., 2017, Analysis of wave propagation in a functionally graded nanobeam resting on visco-Pasternak's foundation, *Theoretical and Applied Mechanics Letters* **7**(3): 145-151.
[28] Arefi M., 2016, Considering the surface effect and nonlocal elasticity in wave propagation of a nano functionally graded piezoelectric rod excited to two-dimensional electric potential and applied voltage, *Applied Mathematics and Mechanics* **37**(3): 289-302.
[29] Arefi M., Zenkour A.M., 2017, Employing the coupled stress components and surface elasticity for nonlocal solution of wave propagation of a functionally graded piezoelectric Love nanorod model, *Journal of Intelligent Material Systems and Structures* **28**(17): 2403-2413.
[30] Arefi M., Soltan Arani A.H., 2018, Higher order shear deformation bending results of a magneto-electro thermoelastic functionally graded nanobeam in thermal, mechanical, electrical, and magnetic environments, *Mechanics Based Design of Structures and Machines* **46**(6): 669-692.
[31] Zenkour A.M., Arefi M., 2017, Nonlocal transient electro thermomechanical vibration and bending analysis of a functionally graded piezoelectric single-layered nanosheet rest on visco-Pasternak foundation, *Journal of Thermal Stresses* **40**(2): 167-184.
[32] Ghorbanpour Arani A., Haghparast E., BabaAkbar-Zarei H., 2017, Vibration analysis of functionally graded nanocomposite plate moving in two directions, *Steel and Composite Structures* **23**(5): 529-541.
[33] Ghorbanpour Arani A., GS Jafari G.S., 2015, Nonlinear vibration analysis of laminated composite Mindlin micro/nano-plates resting on orthotropic Pasternak medium using DQM, *Applied Mathematics and Mechanics* **36**(8): 1033-1044.
[34] Arefi M., Mohammad-Rezaei Bidgoli E., Dimitri R., Tornabene F., 2018, Free vibrations of functionally graded polymer composite nanoplates reinforced with graphene nanoplatelets, *Aerospace Science and Technology* **81**: 108-117.
[35] Arefi M., Pourjamshidian M., Ghorbanpour Arani A., 2017, Application of nonlocal strain gradient theory and various shear deformation theories to nonlinear vibration analysis of sandwich nano-beam with FG-CNTRCs face-sheets in electro-thermal environment, *Applied Physics A* **123**(5): 323.
[36] Arefi M., Zenkour A.M., 2017, Size-dependent vibration and bending analyses of the piezomagnetic three-layer nanobeams, *Applied Physics A* **123**(3): 202.
[37] Arefi M., Zenkour A.M., 2017, Electro-magneto-elastic analysis of a three-layer curved beam, *Smart Structures and Systems* **19**(6): 695-703.
[38] Arefi M., Zenkour A.M., 2016, Employing sinusoidal shear deformation plate theory for transient analysis of three layers sandwich nanoplate integrated with piezo-magnetic face-sheets, *Smart Materials and Structures* **25**: 115040.
[39] Arefi M., Zenkour A.M., 2017, Thermo-electro-mechanical bending behavior of sandwich nanoplate integrated with piezoelectric face-sheets based on trigonometric plate theory, *Composite Structures* **162**: 108-122.
[40] Arefi M., Zenkour A.M., 2017, Thermo-electro-magneto-mechanical bending behavior of size-dependent sandwich piezomagnetic nanoplates, *Mechanics Research Communications* **84**: 27-42.
[41] Arefi M., Zenkour A.M., 2017, Size-dependent free vibration and dynamic analyses of piezo-electro-magnetic sandwich nanoplates resting on viscoelastic foundation, *Physica B : Condensed Matter* **521**: 188-197.
[42] Arefi M., Zamani M.H., Kiani M., 2017, Size-dependent free vibration analysis of three-layered exponentially graded nanoplate with piezomagnetic face-sheets resting on Pasternak's foundation, *Journal of Intelligent Material Systems and Structures* **29**(5): 774-786.
[43] Karamanli A., 2017, Elastostatic analysis of two-directional functionally graded beams using various beam theories and Symmetric Smoothed Particle Hydrodynamics method, *Composites Structures* **160**: 653-669.
[44] Hao D., Wei C., 2016, Dynamic characteristics analysis of bi-directional functionally graded Timoshenko beams, *Composites Structures* **141**: 253-263.
[45] Ghorbanpour Arani A., Haghparast E., BabaAkbar-Zarei H., 2016, Nonlocal vibration of axially moving graphene sheet resting on orthotropic visco-Pasternak foundation under longitudinal magnetic field, *Physica B* **495**: 35-49.
[46] Mohammadimehr M., Rousta Navi B., Ghorbanpour Arani A., 2017, Dynamic stability of modified strain gradient theory sinusoidal viscoelastic piezoelectric polymeric functionally graded single-walled carbon nanotubes reinforced nanocomposite plate considering surface stress and agglomeration effects under hydro-thermo-electro-magneto-mechanical loadings, *Mechanics of Advanced Materials and Structures* **24**(16): 1325-1342.
[47] Shu C., 2000, *Differential Quadrature and its Application in Engineering*, New York, Springer.
[48] Shu C., Du H., 1997, Implementation of clamped and simply supported boundary conditions in the GDQ free vibration analysis of beams and plates, *Journal of Sound and Vibration* **34**: 819-835.
[49] Kim Y.W., 2005, Temperature dependent vibration analysis of functionally graded rectangular plates, *Journal of Sound and Vibration* **284**(3): 531-549.

[50] Ebrahimi F., Ghasemi F., Salari E., 2016, Investigating thermal effects on vibration behavior of temperature-dependent compositionally graded Euler beams with porosities, *Meccanica* **51**(1): 223-249.
[51] Nguyen D.K., Nguyen Q.H., Tran T.T., Bui V.T., 2017, Vibration of bi-dimensional functionally graded Timoshenko beams excited by a moving load, *Acta Mechanica* **228**(1): 141-155.